

EFFICIENT AND FAST REMOVAL OF CADMIUM BY NANOPOWDER MATERIAL FROM AQUEOUS SOLUTION

O. K. AL-DUAIJ*

*Al Imam Mohammad Ibn Saud Islamic University (IMSIU), College of Sciences,
Department of Chemistry, Riyadh 11623, Saudi Arabia.*

In this work we have investigated the removal of cadmium metal ions from synthetic solutions employing zinc oxide nanoparticles prepared by sol-gel method. The structural characterization of the prepared ZnO powder revealed mesoporous particles with hexagonal wurtzite and $109.7\text{ m}^2\cdot\text{g}^{-1}$ surface area. Closed reactor experiments were accomplished to evaluate kinetics, equilibrium, and thermodynamic parameters of the adsorption process. The adsorption process of the removal of cadmium ions was highly initial concentration dependent. A fast equilibrium was attained to achieve a maximum adsorption capacity and the experimental data suited well Langmuir and Freundlich adsorption models. The kinetics pseudo-second-order rate law was found to be in good agreement with the experimental data of the removal.

(Received December 25, 2018; Accepted February 7, 2018)

Keywords: ZnO nanopowder; Characterizations; Adsorption; Cadmium removal

1. Introduction

Heavy metal ions are common in industrial waste waters and are regarded as the main source of water pollution since they are highly soluble in aquatic milieus [1]. Consequently, they are up taken by living organisms that can facilitate their entrance to human bodies through food chains causing grave health maladies. Cadmium, one of the highly toxic heavy metals, can be discharged to the environment from metal production facilities, fossil fuels incineration, electroplating, batteries, pigments and screens factories [2].

Elimination of heavy metals from wastewater can be done by ion exchange, chemical precipitation, liquid extraction or electro-dialysis and membrane filtration. These elimination processes are scarcely employed for small-scale industries owing to their low feasibility and high cost. Actually, removal of these pollutants by adsorption is by far the most pliable and broadly applied route. Moreover, common adsorbents comprise activated carbon, zeolite, coconut shell, manganese or iron oxides and resins used for the uptake of heavy metal ions [3].

Recently, nanomaterials have attracted considerable importance in adsorption processes due their great ability to oust various pollutants from aqueous media [4]. Heavy metals ions removal by nanomaterials has become a focus of water quality research concerns. Nanomaterials have been considered a prospective candidate for wastewater treatment that offers numerous advantages, such as cost effectiveness, enhanced efficiency, and eco-friendliness [5]. Nanoparticulate oxide (ZnO) is used as a photocatalyst for mineralization of toxic organic and inorganic compounds. It is a poor absorber of photons in the solar light due to their band gap is wide (3.2 eV). It is nontoxic and therefore applied for the pollutants uptake from aqueous systems by adsorption.

This work aims to study the operational parameters of the adsorption process of cadmium by ZnO nanoparticles, in particular, initial concentration on Cd^{2+} and temperature. Relevant numerical models such as Langmuir's and Freundlich's adsorption equations are tested. The first and second-order rate equations for describing the kinetics of the Cd^{2+} ions removal are explored. A mechanism for the metal ions adsorption has been proposed.

*Corresponding author: okduaij@yahoo.com

2. Material and Methods

2.1. Material

The Zinc precursor ($\text{Zn}(\text{CH}_3\text{COO})_2 \cdot 2\text{H}_2\text{O}$), absolute CH_3OH (99.99%) and tartaric acid (CHOH-COOH)₂ were procured from Panreac and all of chemicals were used as received. A calculated amount of the zinc salt was dissolved in 0.075 L of CH_3OH and agitated for a half of hour at 450 rpm. The tartaric acid catalyst was dissolved in 0.045 L of distilled water and held for stirring for a half of hour. The tartaric acid solution was added dropwise to the zinc acetate solution and the mixture was subjected to high speed magnetic agitation. A white gel was immediately yielded. The gel was then dried at 358 K for 16 hours to obtain a powder. The powder was finely grinded and annealed in a tubular furnace at 523 K for an hour.

The characteristics of the so-produced nanopowder pores were deduced from the adsorption-desorption isotherms of N_2 at 77 K, realized by a Micromeritics apparatus (ASAP 2020). The pores surface area was computed from the (Brunauer, Emmett and Teller) or BET equation. Whereas the method of t-plot adopted by Lippens and de Boer [6] permit the estimation of the surface area attributes to mesopores and micropores volume. The crystallinity and average particles size of nanopowder were determined by X-ray diffraction patterns. The XRD pattern of the powder was obtained by a D8 Advance Bruker diffractometer equipped with Cu-K α radiation ($\lambda = 1.5406 \text{ \AA}$), scanning angle ranging from 20 to 80° and accelerating voltage about 40 kV. The ZnO nanopowder's morphology was observed by a scanning electron microscope (SEM).

A mass of 1 g cadmium nitrate ($\text{Cd}(\text{NO}_3)_2$) was dissolved in 1L distilled water to prepare a stock solution of Cd^{2+} . Then successive dilutions were processed to obtain experimental solutions at the desired concentration. All chemicals used in this investigation were of analytical grade were purchased from Panreac.

The adsorption experiments of Cd^{2+} on ZnO nanopowder were realized in batch mode reactor at controlled conditions. The experiments were conducted by adding a mass of about 10 mg of adsorbent to 25 ml of Cd^{2+} solution concentration varying from 20 to 140 mg.L^{-1} and a fixed pH value in a 50 ml Erlenmeyer flask to obtain equilibrium isotherms. All flasks were positioned on a multiposition magnetic stirrer to be individually stirred at similar conditions. After 12 h of contact, A volume of about 15 ml of the mixture was sampled from each container after 12 hrs of contact, centrifuged using a Hettich Zentrifugen EBA 20 centrifuge, and then passed through filter- paper. The equilibrium cadmium ion concentration remaining in the filtrate was estimated using an ICP analyzer (Genius, ICP-EOS, Germany).

The maximum adsorbed quantity of Cd^{2+} ion per gram of nanopowder (mg.g^{-1}), q_e , and the percentage of removal was computed using the following equations:

$$q_e = \frac{(C_0 - C_e) * V}{m} \quad (1)$$

$$\% \text{Removal} = \frac{(C_0 - C_e)}{C_0} * 100\% \quad (2)$$

where V and m are respectively, the solution volume in litter and the nanopowder mass in gram. C_0 and C_e are respectively the initial and equilibrium concentrations in mg.L^{-1} , respectively.

2.2. Methods

Once equilibrium was attained between adsorbed metal ions on the ZnO particles and un adsorbed metal ions in solution can be represented by adsorption isotherms. The Langmuir and the empirical Freundlich models were the most broadly utilized isotherm equations for equilibrium data modeling:

$$\frac{C_e}{q_e} = \frac{1}{q_m} C_e + \frac{1}{q_m \cdot K_L} \text{ linear form of Langmuir equation} \quad (3)$$

$$\ln q_e = \frac{1}{n} \ln C_e + \ln K_F \text{ linear form of Freundlich equation} \quad (4)$$

Where q_m is the cadmium ions concentration adsorbed by the adsorbent, which corresponds to the complete coverage of adsorption sites monolayer [7], and K_L Langmuir constant that correspond to the adsorption free energy. The plot of the linear form of Langmuir model (Eq. 3) permit the determination of q_m and K_L values from the slope ($1/q_m$) and the intercept ($1/[q_m \cdot K_L]$), respectively. The Freundlich model constants (K_F and n) are respectively determined from the slope ($1/n$) and the intercept ($\ln K_F$) of the linear plot of $\ln q_e$ versus $\ln C_e$ (Eq. 4). The Freundlich model constants, K_F and n , can be attributed to the strength of adsorbent-adsorbate bond and the bond distribution, respectively [8].

In fact, the kinetic study is generally done using various models. In this investigation only the pseudo-first- and the pseudo-second-order kinetic models were used to predict the adsorption data of Cd^{2+} as a function of time. The first-order kinetics model can be used to model the adsorption process, and its expression is as follows [8]:

$$\ln(q_e - q_t) = \ln(q_e) - k_1 \cdot t \quad (4)$$

where k_1 (min^{-1}) is the adsorption rate constant, q_t ($\text{mg} \cdot \text{g}^{-1}$) is the amount of solute adsorbed as a function of time t (min), which are respectively obtained from the slope and intercept of the linear plots of equation 4. According to Ho and McKay [9], sorption kinetics can be represented by a pseudo-second-order model which expressed as follow:

$$\frac{t}{q_t} = \frac{1}{k_2 \cdot q_e^2} + \frac{t}{q_e} \quad (5)$$

where k_2 is the rate constant of the pseudo-second-order model (in $\text{g} \cdot \text{mg}^{-1} \cdot \text{min}^{-1}$). The value of q_e and k_2 are easily identified graphically from the slope of the linear plot equation 5, respectively.

3. Result and discussion

3.1. Nitrogen Isotherm

Gases adsorption isotherms on solid particles shape affords information on pore size, which is typically considered as micropore, mesopore, or macropore. Fig. 1 shows, the adsorption-desorption isotherm of N_2 at 77 K for ZnO nanopowder, which is obviously of type II, according to the IUPAC classification [10].

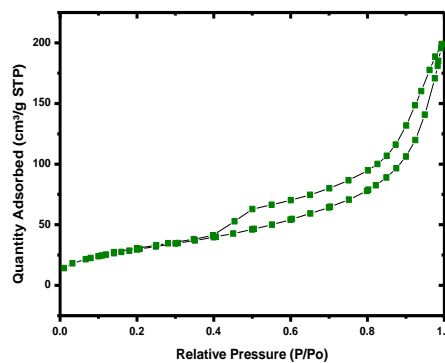


Fig. 1. Nitrogen Adsorption-desorption isotherms of Zinc oxide.

The hysteresis Type H3 features of a mesoporous material and the adsorption is not limited at relative pressure close the unit, signifying a slit-shaped pores [10]. The specific surface area (S_{BET}) is about $109 \text{ m}^2.\text{g}^{-1}$ computed by the BET method and porous volume of about $0.313 \text{ cm}^3.\text{g}^{-1}$. The average pore size value calculated from the BET surface area and the pore volume in the approximation of cylindrical pores is about 9.96 nm .

3.2. Structure and morphology

Fig. 2 (a-b) displays the SEM micrographs obtained for the produced ZnO (a) and calcinated at (b) 250°C . The shape of the nanoparticles shown in the micrographs has changed from a plate shape to spherical shape after calcination. In addition, a small increase in the agglomeration owing to the temperature increase yielding a larger particle sizes [11].

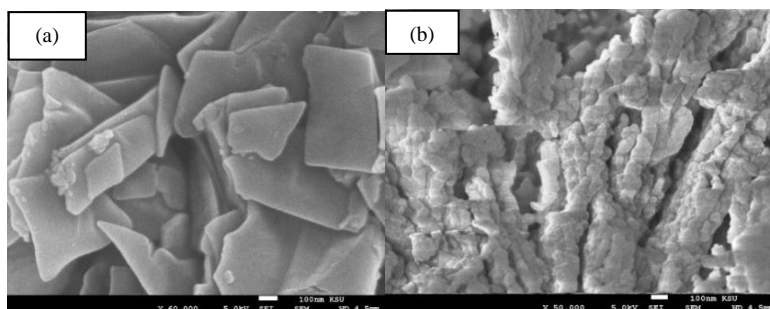


Fig. 2. SEM micrographs of (a) xerogel (b) calcinated ZnO at 250°C

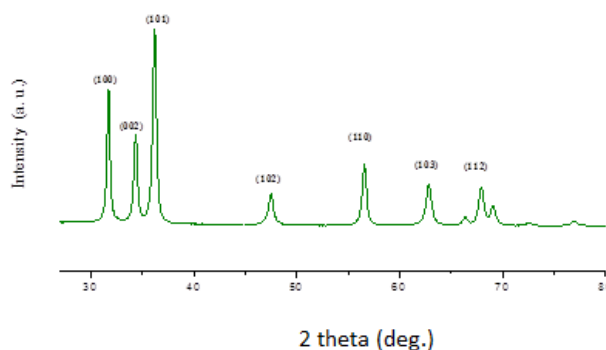


Fig. 3. XRD patterns of ZnO calcinated for 1 hour at 250°C .

Fig. 2 illustrates the XRD patterns of zinc oxide nanoparticles. The findings display broad peaks at positions (31.61, 34.39, 36.11, 47.40, 56.52, 62.72, 66.29, 67.91 and 69.08° as 2θ). The found values are mimic with standard card (JCPDS 36-1451) for ZnO and can be indexed as the hexagonal wurtzite structure. The average crystallite size (D) was found to be equal to 16.12 nm .

3.3. pH effect

The ZnO nanoparticles efficiency to remove cadmium metal ions was inspected at 3–10 pH range and $50 \text{ mg.L}^{-1} \text{ Cd(II)}$ concentrations to speculate the effect of pH on the adsorption process. As can be seen in Fig. 4a sharp drop in the Cd(II) removal efficiency commences beyond $\text{pH} \approx 7$. Therefore all further investigations were carried out at $\text{pH} = 7.0$. As reported earlier [12], a competition between the proton (H^+) and the positive metal ions takes place at low pH leading to lower removal efficiency. Conversely, at higher pH values, the possibility of Cd(OH)^+ and/or Cd(OH)_2 formation [13], that may restrain the removal efficiency is highly possible.

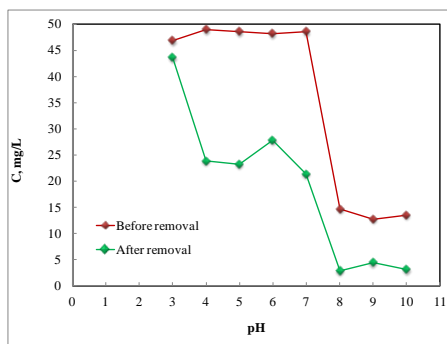


Fig.4. The effect of pH values on the initial concentration of the heavy metal ion solutions

3.4. Heavy metals adsorption study

3.4.1. Kinetic study

Fig. 5 illustrates the sorption of Cd(II) on the nanopowder at 298 K for different time intervals. It is evident that initially there is a sharp rise in the adsorption capacities q_t up to 10 minutes and an equilibrium is almost attained after 75 minutes.

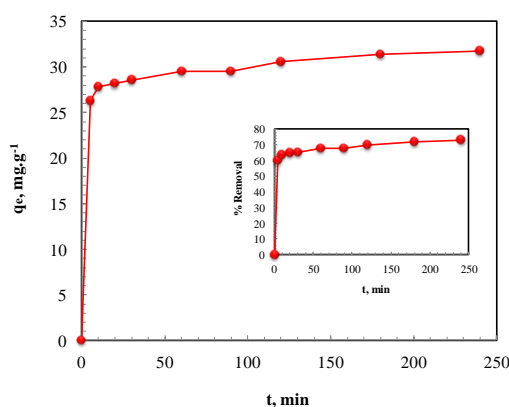


Fig.5. Plot of the adsorption capacity of Cd^{2+} on ZnO nanopowder as a function of time.

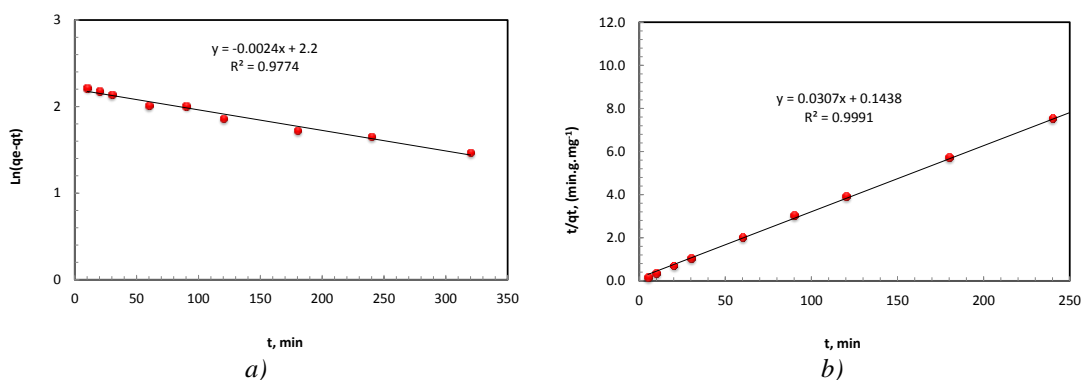


Fig.6: The removal Kinetics of Cd^{2+} on ZnO powder (a) pseudo first order plot and (b) pseudo-second-order plot. Conditions: 298 K, pH = 7, 0.12 g ZnO in 0.2 L of solution 27mg/L.

The pseudo-first order and pseudo-second order kinetics parameters (q_m (cal), K_1 and K_2) with correlation coefficient (r^2) are calculated and viewed on Table 1. The appropriateness of a

kinetic model is verified through the value of the regression coefficient r^2 , shown in table 1. It is clearly that for a pseudo-first order model, the correlation coefficient is about 0.977. In addition, the experimental and theoretically calculated value of q_m are not in good agreement.

Table 1: Rate adsorption constants for the adsorption of Cd^{2+} by the adsorbent

$q_{m(exp)}^a$ (mg/g)	First-order			Second-order		
	$k_1 \times 10^3$ (1/min)	$q_{m(cal)}^b$ (mg/g)	r^2	$k_2 \times 10^3$ (g/(mg.min))	$q_{m(cal)}^b$ (mg/g)	r^2
35.33	2.4	9.03	0.9774	6.55	32.57	0.9991

Therefore, the pseudo-first order kinetics is indeed not suitable for representing the Cd(II) ion adsorption data. In comparison, the use of a pseudo-second order model resulted in obtaining a much better regression coefficients value of 0.9991. Furthermore, the experimental and calculated values of q_m are incredibly close, as indicated in table 1. Accordingly, the pseudo-second order kinetic model is more relevant to the experimental adsorption data of Cd (II) onto the nanopowder material. Likewise, the better fitting of the pseudo-second-order model compared to the pseudo-first-order model for Cd^{2+} adsorption on different adsorbents [14-17] was previously observed.

3.4.2. Equilibrium study

The removal of the toxic Cd^{2+} ions from aqueous solutions is explored at 7.0 ± 0.2 pH and room temperature. This was done by mixing 10 mg of zinc oxide (ZnO) with 25 ml solution of different initial concentration solution varying from 20 to 140 $mg.L^{-1}$ in 50 ml Erlenmeyer flask and stirred at 500 rpm for 12 hours

The graph of Fig.7 demonstrates the adsorption data of the cadmium heavy metal ions by ZnO nanopowder. The linearized Langmuir and Freundlich isotherms of Cd^{2+} (figure 6a and 6b) in solutions are drawn and the estimated model respective parameters (q_m , K_L , K_F and n) with correlation coefficient (r^2) are gathered in Table 2.

Table 2: Equilibrium constants for the removal of heavy metal ions.

T(K)	Langmuir constants			Freundlich constants		
	$q_m(mg.g^{-1})$	$K_L(l.mg^{-1})$	r^2	n	k_f	r^2
298	106.4	0.00635	0.9972	1.687	4.11	0.9813
318	112.4	0.00389	0.9988	1.963	7.35	0.9873
338	121.9	0.00256	0.9927	2.128	10.46	0.9739

Due to the considerably high values of the regression coefficient r^2 , the Langmuir model better fits the adsorption equilibrium data. It is apparent from that the adsorption of ZnO for Cd(II) is in direct proportion with the temperature, i.e. the adsorption capacity of Cd(II) is about 121.9 $mg.g^{-1}$, which was significantly higher than the values 106.4 and 112.4 $mg.g^{-1}$ observed for the two other operational temperatures. The n values greater than 1 are indicative of a Langmuir process and of very weak interactions between molecules of solute. Moreover, the values of Freundlich constants increase proportionally to the temperature.

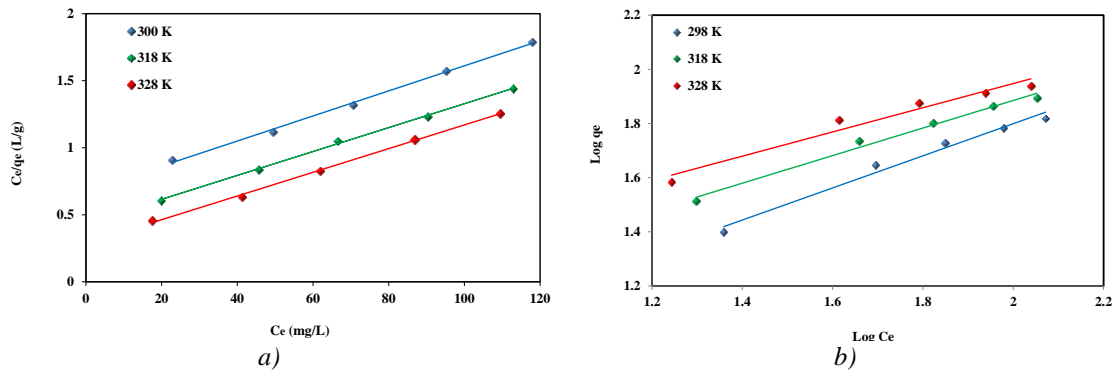
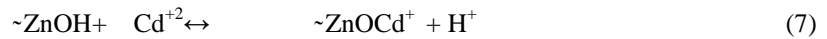


Fig.7. Linearized adsorption equilibrium isotherms of Cd^{2+} at different temperatures by adsorbent nanopowder (a) Langmuir linear equation, (b) Freundlich linear equation.

3.4.3. Mechanism of adsorption

Mosayebi and Azizian [18] proposed a mechanism for the elimination of Cu^{2+} by ZnO and $\text{Zn}(\text{OH})_2$ based on the effect of the solution pH. As the solution pH approaches the pH_{pzc} a decline of the repulsive interaction between the adsorbate and adsorbent surface leading to an enhancement of the removal efficiency of the positive ions. The same argument holds for the Cd^{2+} ions and a complex formation [18] can be suggested:



The equilibrium will be shifted to the right as the pH is increased.

The cadmium ions uptake can be governed by a mass transfer in the boundary film of liquid or an intra-particle mass transfer. The external mass transfer coefficient, β_L (m.s^{-1}) of Cd^{2+} in the boundary film, may be estimated using the equation: [19, 20].

$$\ln\left(\frac{C_t}{C_0} - \frac{1}{1+m.K_a}\right) = \ln\left(\frac{m.K_a}{1+m.K_a}\right) - \left(\frac{1+m.K_a}{m.K_a}\right) \cdot \beta_L \cdot S_s \cdot t \quad (8)$$

where C_t and C_0 (both in mg.L^{-1}) are the metal ion concentration at time t and zero respectively, K_a (L.g^{-1}) is a constant is the product of the Langmuir constants: $K_a = Q_0/b$; m (g) is the adsorbent mass, and S_s is the adsorbent surface area ($\text{m}^2.\text{g}^{-1}$). A straight line in $\ln[(C_t/C_0 - 1/(1+m.K_a))]$ versus t plot is required to prove the reliability of model.

The adsorbed ions may get transported from the solution bulk to the solid phase through intra-particle diffusion/transport process. The intra-particle diffusion is the limiting step in many adsorption process.

The possibility of intra-particle diffusion is determined using the Weber and Morris diffusion mode [21,22].

$$q_t = k_{\text{dif}} \cdot t^{1/2} + C \quad (9)$$

where C is the intercept and k_{dif} is the intra-particle diffusion rate constant. The k_{dif} for the examined adsorbent is calculated from the slope of the plot (Figure 8). The validity of these models is thereafter discussed. The linear relationship between $\ln[(C_t/C_0 - 1/(1+m.K_a))]$ and t usually support the mass transfer rate model. As can be seen from the plot the data did not provide a linear plot, indicating the invalidity of this model. The values of regression coefficient calculated from Eq. (9) for ZnO nanopowder is about 0.76. This means that the uptake of cadmium ions at the tested adsorbent sites is not governed by liquid phase mass transfer rate. Instead, the uptake of Cd^{2+} at the surface of the adsorbent may be controlled by the intra-particle diffusion kinetic model, since, the values of q_t are found to be linearly correlated with $t^{1/2}$ -values. Besides, the regression

coefficient value is equal to 0.9883 signifying the applicability of this model. The intra-particle diffusion plot is shown in Fig. 9. Main parameters of this model are determined and gathered in Table 3. The values of intercept (i.e. C, Table 3) give an idea about the boundary layer thickness. The larger intercept the greater is the boundary layer effect.

Table 3. Kinetic parameters for the Cd^{2+} ions adsorption onto ZnO nanoparticles based on intraparticle diffusion model

Intraparticle diffusion equation Parameters		
k_{diff} , $\text{mg/g.min}^{1/2}$	C	r^2
19.023	1.9559	0.9883

The Weber–Morris intraparticle diffusion model has often been used to decide whether intraparticle diffusion is the rate-limiting step [23,25] or not. According to the model, if the intra-particle diffusion is the only rate-determining step, then the plot of q_t versus $t^{0.5}$ should pass through the origin ($C = 0$). But in this case, the lines did not pass through the origin confirming that intraparticle diffusion is not the sole rate governing step [26].

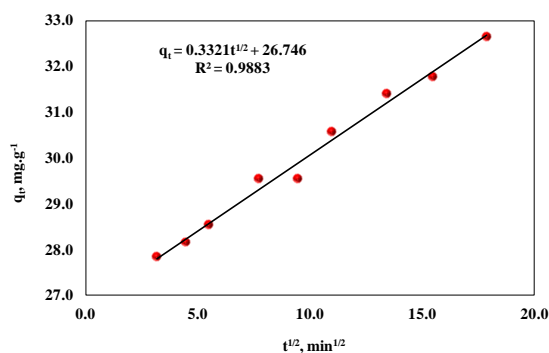


Fig.7. q_t versus $t^{1/2}$ plot for the intraparticle diffusion

From the tabulated results (Table 3), it can be seen that the diffusion rate is very low due to the smaller pores accessible for diffusion as the Cd^{2+} ions previously diffuse into the inner structure of nanoparticles. Also the constant related to the boundary layer thickness (C) is large showing greater boundary layer effects [27].

4. Comparison of Cd (II) Adsorption Capacity with Different Adsorbents

The ability of ZnO nanoparticles to remove Cd^{2+} ions was contrasted with that of some nano-adsorbents, reported in literatures as listed in Table 4. The adsorbent applied in the present work revealed higher adsorption capacity than other adsorbents, demonstrating that the ZnO is a promising adsorbent of Cd^{2+} ions from water and wastewater.

Table 4: A Comparison of ZnO adsorption capacity with some nano-adsorbents for cadmium (II)

Adsorbent	$q_e(\text{mg}\cdot\text{g}^{-1})$	Temp. (K)	Ref.
Milled goethite	125	298	[16]
Ni (15 wt%)-doped $\alpha\text{-Fe}_2\text{O}_3$	90.91	328	[17]
Carbon nanotubes	11.00	298	[28]
Nano $\text{NH}_2\text{-MCM-41}$	18.25	298	[29]
CuFe_2O_4 nano-particles	17.54	298	[30]
Magnetic Graphene Oxide	91.29	298	[31]
ZnO	106	298	Present work
ZnO	112	318	Present work
ZnO	121	328	Present work

5. Conclusions

To sum up that, a suitable nanomaterial was prepared by flash sol-gel method and identified as an effective adsorbent for of cadmium metal ion from aqueous solutions. The equilibrium adsorption data are in good consistency with the Langmuir and Freundlich models, and the adsorbent higher tendency for the uptake of Cd^{2+} at elevated temperature (i.e. $122 \text{ mg}\cdot\text{L}^{-1}$ for Cd^{2+} at 338 K).

Furthermore, it was established that a second-order rate model well mimics the kinetic data for the removal cadmium ions. Temperature is a determinant factor for the removal of Cd^{2+} . A mechanism based on mass transfer principles has been anticipated.

References

- [1] S. Babel, T. A. Kurniawan Chemosphere **54**,951 (2004)
- [2] K.H. Boparai, M. Joseph, D.M. O'Carroll, J. Hazard. Mater.**186**,458 (2011).
- [3] J. W. Patterson, "Industrial Wastewater Treatment Technology", (2nd edition, Butterworth Heinemann, London, 1985.
- [4] K.S. Rao, M. Mohapatra, S. Anand, P. Venkateswarlu, International Journal of Engineering, Science and Technology.**2**(7), 81(2010).
- [5] P. R.Grossel, D. L. Sparks, C. C. Ainsworth, Environ. Sci. Technol. **28** 1422(1994).
- [6] B.C. Lippens, J.H.De Boer, J. Catalysis**4**,319 (1965).
- [7] C.P. Huang, E.H. Smith, Chemistry in water reuse, Ann Arbor Science Publishers, Ann Arbor, Michigan, 2 (1981).
- [8] V.K. Gupta, S. Sharma, I.S. Yadau, M. Dinesh, Journal Chemical Technology and Bio-thechnol.**71**,180 (1998).
- [9] Y.S.Ho, G.Mckay, Chemical Engineering Journal**70**, 115 (1998).
- [10] F. Rouquerol, J Rouquerol, K. Sing, Adsorption by Powder and Porous Solids: Principles, Methodology an Applications, Academic Press.1999.
- [11] J. Zhang, X.Xiao, J. Nan, J. Hazardous Mat. **176**, 617(2010).
- [12] L. Dong, A. Zhu, H. Ma, Y. Qiu, J. Zhao, J. Environ. Sci. **22**(2), 225 (2010).
- [13] G. Yang, L. Tang, X. Lei, G. Zeng, Y. Cai, X. Wei, Y. Zhou, S. Li, Y. Fang, Y. Zhang, Appl. Surf.Sci.**292**,710 (2014).
- [14] A.B. Perez-Marin, V.M. Zapata, J.F. Ortuno, M. Aguilar, J. Saez, M. Llorens, J. Hazard. Mater.**139**,122 (2007).
- [15] H. Javadian, F. Ghorbani, H. Tayebi, S. M. H. Asl. Arabian Journal of Chemistry **8**, 837 (2015).
- [16] L. Khezami, Mohamed OuldM'hamed, O.M. Lemine, M. Bououdina, AbdelbassetBessadok-Jemai, Desalination and Water Treatment **57**,6531 (2016).
- [17] M. O. M'hamed, L. Khezami, A. G Alshammari, SM Ould-Mame, I Ghiloufi, OM Lemine Water Science & Technology, **72**,608 (2015).

- [18] E. Mosayebi, S. Azizian, *Journal of Molecular Liquids* **214**,384(2016).
- [19] C. Faur-Brasquet, Z. Reddad, K. Kadirvelu, P. Le Cloirec, *Appl. Surf. Sci.* **196**,356 (2002).
- [20] C. Faur-Brasquet, Z. Reddad, K. Kadirvelu, P. Le Cloirec, *Appl. Surf. Sci.* **196**,356 (2002).
- [21] M. N. Sahmoune, N. Ouazene, *Environmental Progress & Sustainable Energy*, **31**(4),597 (2012).
- [22] B.H. Hameed, J.M. Salman, A.L. Ahmad, *J. Hazard. Mater.* **163**,121 (2009).
- [23] S.I.H. Taqvi, S.M. Hasany, M.Q. Bhanger, *J. Hazard. Mater.* **14**,37 (2007).
- [24] F.C. Wu, R.L. Tseng, R.S. Juang, *Chem. Eng. J.* **153**,1 (2009).
- [25] D. Kavitha, C. Namasivayam, *Bioresour. Technol.* **98**,14 (2007).
- [26] A. Ozcan, A.S. Ozcan, O. Gok, Adsorption kinetics and isotherms of anionic dye of reactive blue 19 from aqueous solutions onto DTMA-sepiolite, in: A.A. Lewinsky (Ed.), *Hazardous Materials and Wastewater—Treatment, Removal and Analysis*, Nova Science Publishers, New York, 2007.
- [27] M.Yazdani, T. Tuutijärvi, A. Bhatnagar, R. Vahala, *Journal of Molecular Liquids* **214**,149 (2016).
- [28] N. B. Milosavljevi, M. Risti, A. A. Peric-Grujic, J. M. Filipovic, S. B. Strbac, Z. Lj. Rakocevic, M. T. K. Krusic, *Colloids and Surfaces A: Physicochem. Eng. Aspects* **388**,59 (2011).
- [29] Y H Li, S G Wang, Z K Luan, J Ding, C L Xu, D H.Wu, *Carbon* **41**(5),1057 (2003).
- [30] Y. J. Tu, C. F. You and C. K. Chang, *Journal of Hazardous Materials* **235– 236**,116 (2012).
- [31] A Heidari, H Younesi, Z Mehraban, *Chemical Engineering Journal* **153**(1-3), 70 (2009).